

Impact of the Trivedi Effect® on the Physicochemical Properties of Antimony

Branton A¹, Trivedi MK¹, Trivedi D¹, Nayak G¹ and Jana S^{2,*}

¹Trivedi Global, Inc., Henderson, USA

²Trivedi Science Research Laboratory Pvt. Ltd., Thane (W), India

***Corresponding author:** Snehasis Jana, Trivedi Science Research Laboratory Pvt. Ltd.,

Thane (W), Maharashtra, India, Tel: +91-022-25811234; Email: publication@trivedieffect.com

Research Article

Volume 3 Issue 4

Received Date: September 18, 2019

Published Date: October 23, 2019

Abstract

The objective of this scientific research work was to evaluate the impact of the Trivedi Effect® on the physicochemical properties of antimony (Sb) powder using modern analytical techniques. Antimony is a chemical element, which has many applications in the medicine, cosmetics, metal, and electronic industry. The powder sample was divided into two parts, one part of antimony was considered as control sample, while second part received the Trivedi Effect®-Consciousness Energy Healing Treatment remotely by a famous Biofield Energy Healer, Alice Branton and termed as a Biofield Energy Treated sample. The PXRD peak intensities and crystallite sizes of the treated antimony were significantly altered ranging from 3.43% to 52.58% and -17.22% to 166.4%, respectively compared to the control sample. However, the average crystallite size of the treated sample was significantly increased by 25.96% compared with the control sample. The particle size values in the treated antimony were significantly increased by 51.60% (d_{10}), 20.17% (d_{50}), 35.34% (d_{90}), and 26.32% {D(4,3)}, respectively compared to the control sample. Therefore, the specific surface area of the treated antimony powder was significantly decreased by 27% compared with the control sample. The total weight loss was decreased by 4.43%; however, the residual amount was significantly increased by 15.04% in the treated antimony compared with the control sample. The maximum thermal degradation temperature (T_{max}) of the 1st peak in the treated sample was decreased by 4.35%, whereas the T_{max} of the 2nd peak in the treated sample was significantly increased by 5.41% compared with the control sample. The results concluded that the Trivedi Effect®-Consciousness Energy Healing Treatment might lead to generate a new polymorphic form of antimony which would improve the physicochemical and thermal stability compared with the untreated sample. The treated antimony would be very useful for designing better pharmaceutical and cosmetic formulations as antimonials, meglumine antimoniate, antiprotozoal drugs, anti-schistosomal, veterinary preparations, nourishing or conditioner of keratinized tissues. It would also be useful for the heavy industries for the production of alloys, fire retardant, solders, electrical cables, bullets, plain bearings, microelectronics, etc.

Keywords: Antimony; The Trivedi Effect®; Consciousness Energy Healing Treatment; PXRD analysis; Particle size; Thermal degradation temperature

Introduction

Antimony (Sb) is a chemical element, found in nature mainly in the form of sulfide mineral stibnite (Sb_2S_3). Four allotropes of antimony are established till now are a stable metallic form and three metastable forms (black, yellow, and explosive). Antimony has two stable isotopes: ^{121}Sb (57.36%) and ^{123}Sb (42.64%), 35 radioisotopes, and 29 metastable states have been characterized [1]. In the metal industries antimony used for making of alloy with lead and tin and the lead antimony plates in lead-acid batteries. The lead, tin and antimony alloy have improved properties for solders, electrical cables, bullets, and plain bearings. Fire retardants contain the antimony compounds as a prominent additive for chlorine and bromine, which found in many commercial and domestic products. It is used as a stabilizer and a catalyst for the production of polyethylene terephthalate. Antimony also has an emerging demand in microelectronics [2-5]. Antimony has been known since ancient times and were powdered for use as medicine and cosmetics, i.e., antimonials (emetics), meglumine antimoniate, antiprotozoal drugs, anti-schistosomal, several veterinary preparations (anthiomaline and skin conditioner in ruminants), nourishing or conditioner of keratinized tissues [2,6]. It is toxic by inhalation and ingestion. Antimony on prolonged skin contact may cause dermatitis. It is denser than water, insoluble in water, and slightly oxidized in the air [2,7].

Physicochemical properties of a substance play a crucial role in manufacturing and other industrial purposes. It was experimentally proved that Biofield Energy Healing Treatment (i.e., the Trivedi Effect®) has a significant impact on the physicochemical properties of many substances [8-11]. The Trivedi Effect® is a natural and only scientifically proven phenomenon in which a person can harness this inherently intelligent energy and transmit it anywhere on the planet through the possible mediation of neutrinos [12]. A unique energy field exists surrounding the every living organism's body known as Biofield Energy, which is infinite, para-dimensional electromagnetic field. Biofield based Energy Healing Therapies have been reported to have significant outcomes against various disease conditions [13]. National Institute of Health/National Center for Complementary and Alternative Medicine recommend and included the Energy therapy under Complementary

and Alternative Medicine category that has been accepted by the most of the U.S. population with several advantages [14,15]. Many experiments were scientifically performed in order to prove the impact of the Trivedi Effect® on the non-living and living object(s). The Trivedi Effect® was proved with significantly outcome in various field of science, i.e. metals and ceramic [16-18], organic compounds [19,20], nutraceuticals [21,22], pharmaceuticals [23,24], cancer cells [25,26], microorganisms [27,28], and crops [29,30]. Therefore, this study was designed to determine the impact of the Trivedi Effect®-Consciousness Energy Healing Treatment on the physicochemical, and thermal properties of antimony powder using powder X-ray diffraction (PXRD), particle size analysis (PSA), and thermogravimetric analysis (TGA)/ differential thermogravimetric analysis (DTG).

Materials and Methods

Chemicals and Reagents

The test sample antimony (Sb) powder was purchased from Parshwamani Metals, Mumbai, India. All other chemicals used during the experiments were of analytical grade purchased in India.

Consciousness Energy Healing Treatment Strategies

The antimony powder sample was divided into two parts. One part of the powder sample was considered as a control sample where no Biofield Energy Treatment was provided. However, the second part of antimony powder was received the Trivedi Effect®-Consciousness Energy Healing Treatment remotely under standard laboratory conditions for 3 minutes and known as the Biofield Energy Treated antimony sample. The Biofield Energy Treatment was provided by the renowned Biofield Energy Healer, Alice Branton (USA), to the test sample. Further, the control sample was treated by a "sham" healer, who did not have any knowledge about the Biofield Energy Treatment. After that, both the samples were kept in sealed conditions and characterized using sophisticated analytical techniques.

Characterization

The PXRD analysis of antimony sample was achieved with the help of Rigaku MiniFlex-II Desktop X-ray

diffractometer (Japan) [31-37]. The average crystallite size of antimony was calculated using the Scherrer's formula (1)

$$G = k\lambda / \beta \cos\theta \quad (1)$$

Where G = crystallite size (nm), k = dimensionless shape factor, λ = radiation wavelength, β = full-width half maximum, and θ = Bragg angle [38].

The PSD analysis of antimony was performed with the help Malvern Mastersizer 2000, from the UK using the wet method. Similarly, the TGA/DTG was performed with the help of TGA Q50 TA instruments maintain a nitrogen gas environment [39,40].

The % change in peak intensity, crystallite size, specific surface area (SSA), particle size, the maximum thermal degradation temperature (T_{max}) and weight loss of the Biofield Energy Treated antimony was calculated compared with the control sample using the following equation 2:

$$\% \text{ Change} = \frac{[\text{Treated} - \text{Control}]}{\text{Control}} \times 100 \quad (2)$$

Results and Discussion

Powder X-ray Diffraction (PXRD) Analysis

The PXRD diffractograms of the antimony powder were showed sharp and intense peaks (Figure 1) indicated that both the samples were crystalline in nature. The PXRD diffractograms of the samples showed the highest peak intensity at 2θ equal to 28.7° (Table 1, entry 2). All the peak intensities of the treated antimony were significantly decreased altered ranging from 3.43% to 52.58% compared to the control sample (Table 1, entry 1-13). The crystallite sizes of the treated antimony were significantly altered ranging from -17.22% to 166.4% compared to the control sample (Table 1, entry 1-13). However, the average crystallite size of the treated antimony was significantly increased by 25.96% compared with the control sample.

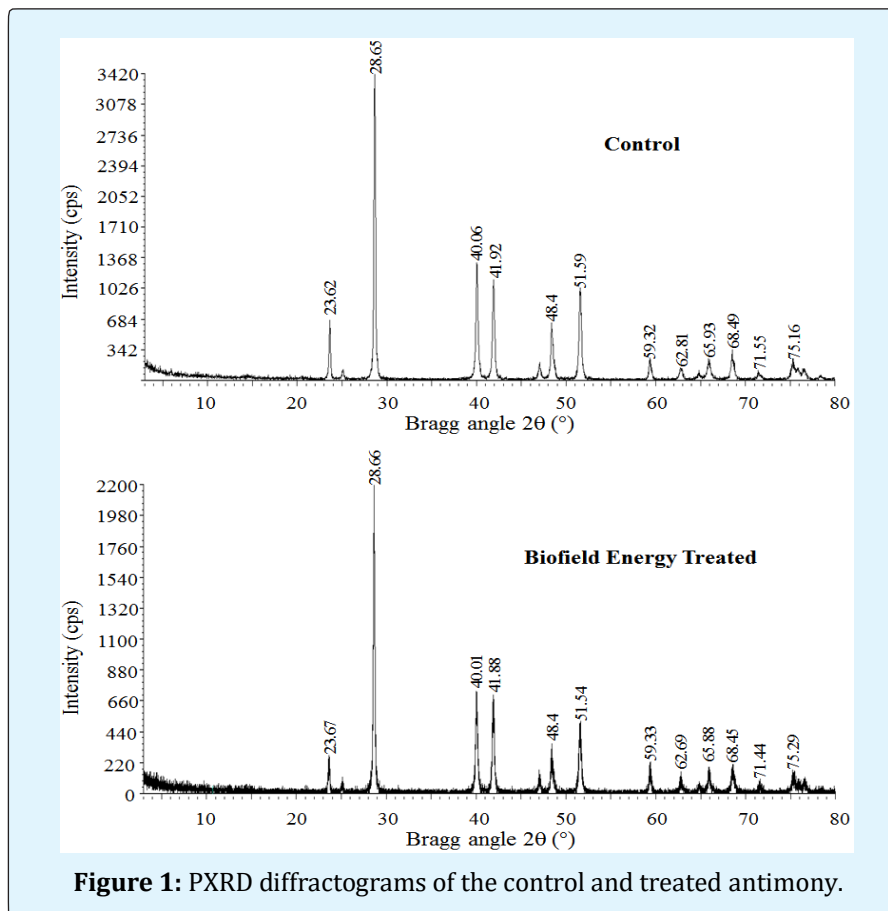


Figure 1: PXRD diffractograms of the control and treated antimony.

Entry No.	Bragg angle ($^{\circ}2\theta$)		Peak Intensity (%)			Crystallite size (G, nm)		
	Control	Treated	Control	Treated	% Change *	Control	Treated	% Change *
1	23.62	23.67	100.00	54.20	-45.80	496.00	430.00	-13.31
2	28.65	28.66	583.00	563.00	-3.43	488.00	479.00	-1.84
3	40.06	40.01	301.00	246.00	-18.27	393.00	352.00	-10.43
4	41.92	41.88	247.00	225.00	-8.91	414.00	351.00	-15.22
5	48.40	48.40	159.00	110.00	-30.82	437.00	387.00	-11.44
6	51.59	51.54	260.00	194.00	-25.38	395.00	327.00	-17.22
7	59.32	59.33	53.10	49.90	-6.03	353.00	447.00	26.63
8	62.81	62.69	34.00	25.70	-24.41	262.00	349.00	33.21
9	64.82	64.85	16.60	10.40	-37.35	256.00	678.00	164.84
10	65.93	65.88	64.00	57.90	-9.53	249.00	421.00	69.08
11	68.49	68.45	82.00	72.00	-12.20	267.00	330.00	23.60
12	71.55	71.44	18.80	13.60	-27.66	250.00	666.00	166.40
13	75.16	75.29	97.00	46.00	-52.58	120.00	300.00	150.00
14	Average crystallite size					336.92	424.38	25.96

Table 1: PXRD data for the control and treated antimony.

*denotes the percentage change in the peak intensity and crystallite size of treated sample with respect to the control sample.

The variations in the crystallite sizes and peak intensities would have modified the crystal morphology of the treated antimony compared to the control sample. The peak intensity of each diffraction face on the crystalline compound changes according to the crystal morphology [36], and alterations in the PXRD pattern provide the proof of polymorphic transitions [37,38]. Therefore, it was expected a new polymorphic form of antimony might have produced due to Trivedi Effect®-Consciousness Energy Healing Treatment probably *via* the mediation of neutrino oscillation [12]. Different polymorphic forms of pharmaceuticals have the significant effects on the thermodynamic and physicochemical properties like melting point, energy, stability, and especially solubility, which are different from the original one [39, 40]. Thus, it can be assumed that the Trivedi Effect® Treated antimony would be better for designing novel nutraceutical or pharmaceutical formulation and also for the other industrial applications.

Particle Size Analysis (PSA)

The particle size distribution analysis of both the

control and Biofield Energy Treated antimony powder were performed, and the data are presented in Table 2. The particle size values in the Biofield Energy Treated antimony were significantly increased at d_{10} , d_{50} , d_{90} , and $D(4,3)$ by 51.60%, 20.17%, 35.34%, and 26.32%, respectively compared to the control sample. Therefore, the specific surface area of Biofield Energy Treated antimony powder (0.619 m^2/g) was significantly decreased by 27% compared with the control sample (0.848 m^2/g). As per the results, it was assumed that the Trivedi Effect®-Consciousness Energy Healing Treatment might be acting like an external force for decreasing the internal energy; hence significantly increased the particle size and decreased the surface area of antimony compared to the control sample. The increased particle size of the antimony powder may help in enhancing the appearance, shape, and flowability [41,42]. Thus, the Biofield Energy Treatment might be used as a measure to improve the appearance, shape, and powder flowability of antimony. Thus, the treated antimony would be better for designing better nutraceutical or pharmaceutical formulation and also useful for the other industrial applications.

Parameter	d_{10} (μm)	d_{50} (μm)	d_{90} (μm)	$D(4,3)$ (μm)	SSA (m^2/g)
Control	3.04	11.54	45.39	19.43	0.848
Biofield Treated	4.60	13.87	61.43	24.54	0.619
Percent change* (%)	51.60	20.17	35.34	26.32	-27.00

Table 2: The particle size distribution of the control and treated antimony.

d_{10} , d_{50} , and d_{90} : particle diameter corresponding to 10%, 50%, and 90% of the cumulative distribution, $D(4,3)$: the average mass-volume diameter, and SSA: the specific surface area. *denotes the percentage change in the particle size distribution of the treated sample with respect to the control sample.

Thermal Gravimetric Analysis (TGA) / Differential Thermogravimetric Analysis (DTG)

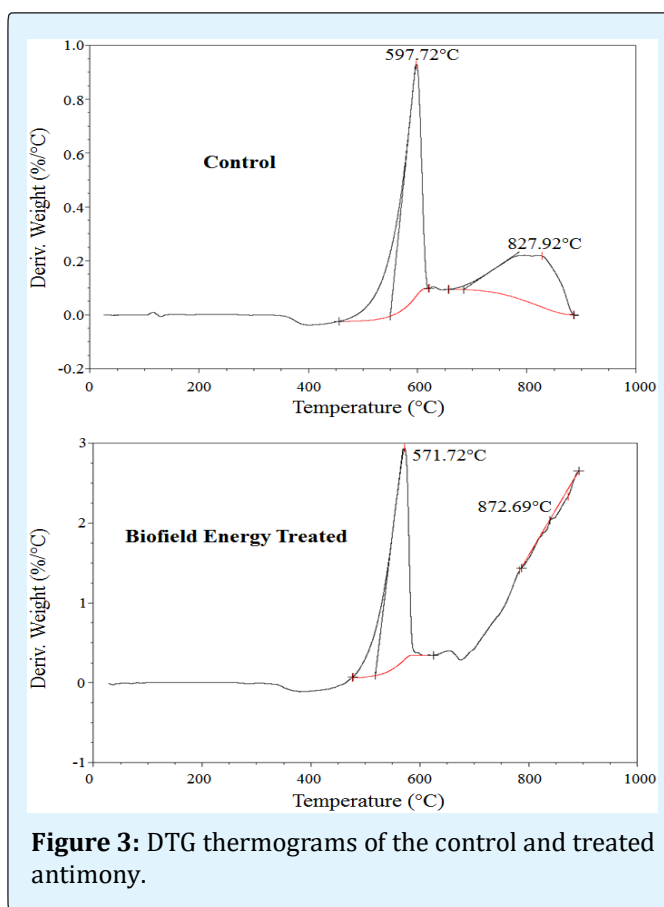
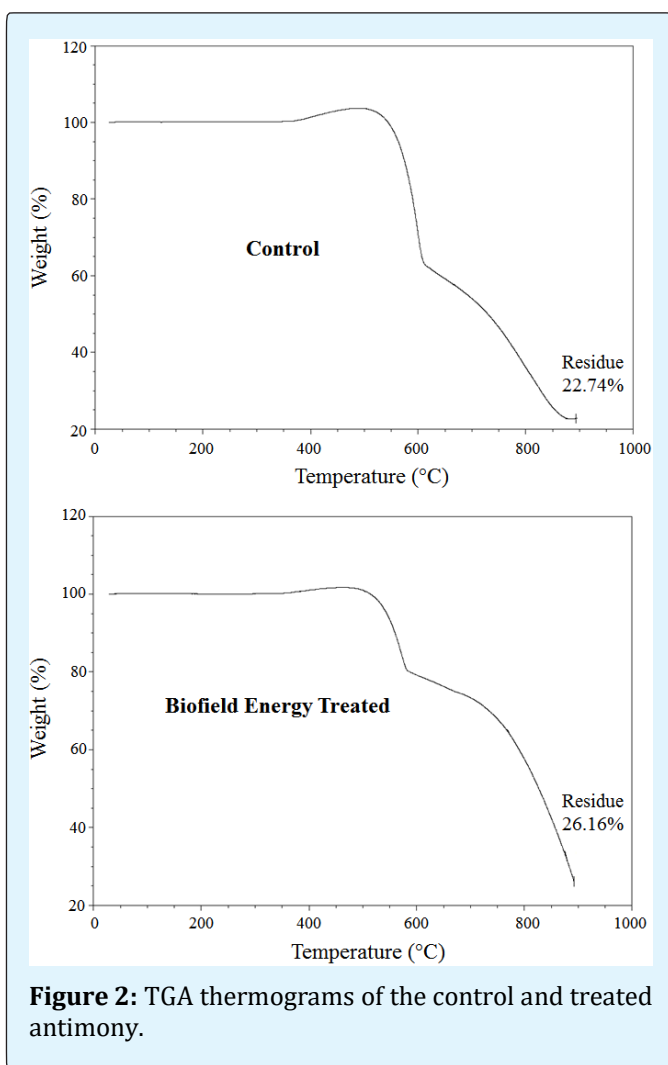
The TGA thermograms of both the samples showed two steps of thermal degradation (Figure 2). The total weight loss in Biofield Energy Treated antimony was

decreased by 4.43% compared with the control sample (Table 3). Therefore, the residue amount was significantly increased by 15.04% in the Biofield Energy Treated antimony compared to the control sample (Table 3).

Sample	TGA		DTG; T _{max} (°C)	
	Total weight loss (%)	Residue %	1 st Peak	2 nd Peak
Control	77.26	22.74	597.72	827.92
Biofield Energy Treated	73.84	26.16	571.72	872.69
% Change*	-4.43	15.04	-4.35	5.41

Table 3: TGA/DTG data of the control and treated samples of antimony.

*denotes the percentage change of the treated sample with respect to the control sample, T_{max} = the temperature at which maximum weight loss takes place in TG or peak temperature in DTG.



The DTG thermogram of the control and Biofield Energy Treated antimony sample exhibited two peaks (Figure 3). The maximum thermal degradation temperature (T_{max}) of the 1st peak in the treated sample

was decreased by 4.35% compared with the control sample (Table 3). However, the T_{max} of the 2nd peak in the Biofield Energy Treated sample was significantly increased by 5.41% compared with the control sample (Table 3). Overall, TGA/DTG revealed that the thermal stability of the Biofield Energy Treated antimony was significantly improved compared with the control sample.

Conclusions

The Trivedi Effect®-Consciousness Energy Healing Treatment showed significant effects on the peak intensities, crystallite size, particle size, surface area, and thermal properties of antimony powder. The PXRD peak intensities of the Biofield Energy Treated antimony were significantly altered ranging from 3.43% to 52.58% compared to the control sample. Similarly, the crystallite sizes of the Biofield Energy Treated sample were significantly altered ranging from -17.22% to 166.4% compared to the control sample. However, the average crystallite size of the Biofield Energy Treated sample was significantly increased by 25.96% compared with the control sample. The particle size values in the treated antimony were significantly increased at d_{10} , d_{50} , d_{90} , and $D(4,3)$ by 51.60%, 20.17%, 35.34%, and 26.32%, respectively compared to the control sample. Therefore, the specific surface area of the Biofield Energy Treated antimony powder was significantly decreased by 27% compared with the control sample. The total weight loss was decreased by 4.43%; whereas, the residual amount was significantly increased by 15.04% in the Biofield Energy Treated antimony compared with the control sample. The T_{max} of the 1st peak in the Biofield Energy Treated sample was decreased by 4.35%, whereas the T_{max} of the 2nd peak in the Biofield Energy Treated sample was significantly increased by 5.41% compared with the control sample. The results concluded that the Trivedi Effect®-Consciousness Energy Healing Treatment might lead to generate a new polymorphic form of antimony which would improve the appearance, shape, powder flowability, and thermal stability compared with the untreated sample. The Trivedi Effect Treated antimony would be very useful for designing better pharmaceutical and cosmetic formulations as antimonials (emetics), meglumine antimoniate, antiprotozoal drugs, anti-schistosomal, veterinary preparations (anthiomaline and skin conditioner in ruminants), nourishing or conditioner of keratinized tissues. It would also be useful for the heavy industries for the production of alloys, fire retardant, solders, electrical cables, bullets, plain bearings, microelectronics, etc.

Acknowledgements

The authors are grateful to Central Leather Research Institute, SIPRA Lab. Ltd., Trivedi Science, Trivedi Global, Inc., Trivedi Testimonials, and Trivedi Master Wellness for their assistance and support during this work.

References

1. Audi G, Bersillon O, Blachot J, Wapstra AH (2003) The NUBASE evaluation of nuclear and decay properties. *Nuclear Physics A* 729(1): 3-128.
2. Antimony.
3. Ipser H, Flandorfer H, Luef Ch, Schmetterer C, Saeed U (2007) Thermodynamics and phase diagrams of lead-free solder materials. *J Mater Sci Mater Electron* 18(1-3): 3-17.
4. John WH (1973) Mass spectrometric studies of flame inhibition: Analysis of antimony trihalides in flames. *Combustion and Flame* 21(1): 49-54.
5. O'Mara, William C, Robert BH, Philip HL (1990) Handbook of semiconductor silicon technology. 1st (Edn.), William Andrew, pp: 815.
6. Organisation Mondiale de la Sante (1995) Drugs used in parasitic diseases. pp: 19-21.
7. Antimony compound.
8. Trivedi MK, Branton A, Trivedi D, Nayak G, Sethi KK, et al. (2016) Determination of isotopic abundance ratio of biofield energy treated 1,4-dichlorobenzene using gas chromatography-mass spectrometry (GC-MS). *Modern Chemistry* 4(3): 30-37.
9. Trivedi MK, Tallapragada RM (2008) A transcendental to changing metal powder characteristics. *Metal Powder Report* 63(9): 22-28.
10. Dabhade VV, Tallapragada RMR, Trivedi MK (2009) Effect of external energy on the atomic, crystalline, and powder characteristics of antimony and bismuth powders. *Bulletin of Materials Science* 32(5): 471-479.
11. Trivedi MK, Nayak G, Patil S, Tallapragada RM, Latiyal O (2015) Evaluation of biofield treatment on physical, atomic and structural characteristics of manganese (II, III) oxide. *J Material Sci Eng* 4(4): 177.

12. Trivedi MK, Mohan TRR (2016) Biofield energy signals, energy transmission and neutrinos. *American Journal of Modern Physics* 5(6): 172-176.
13. Rubik B, Muehsam D, Hammerschlag R, Jain S (2015) Biofield science and healing: history, terminology, and concepts. *Glob Adv Health Med* 4(Suppl): 8-14.
14. Barnes PM, Bloom B, Nahin RL (2008) Complementary and alternative medicine use among adults and children: United States, 2007. *Natl Health Stat Report* 10(12): 1-23.
15. Koithan M (2009) Introducing complementary and alternative therapies. *J Nurse Pract* 5(1): 18-20.
16. Trivedi MK, Tallapragada RM, Branton A, Trivedi D, Nayak G, et al. (2015) Evaluation of atomic, physical, and thermal properties of bismuth oxide powder: An impact of biofield energy treatment. *American Journal of Nano Research and Applications* 3(6): 94-98.
17. Trivedi MK, Nayak G, Patil S, Tallapragada RM, Latiyal O, et al. (2015) Characterization of physical and structural properties of brass powder after biofield treatment. *J Powder Metall Min* 4(1): 134.
18. Trivedi MK, Nayak G, Patil S, Tallapragada RM, Latiyal O, et al. (2015) Studies of the atomic and crystalline characteristics of ceramic oxide nano powders after bio field treatment. *Ind Eng Manage* 4(2): 1-6.
19. Trivedi MK, Branton A, Trivedi D, Nayak G, Panda P, et al. (2016) Determination of isotopic abundance of $^{13}\text{C}/^{12}\text{C}$ or $^2\text{H}/^1\text{H}$ and $^{18}\text{O}/^{16}\text{O}$ in biofield energy treated 1-chloro-3-nitrobenzene (3-CNB) using gas chromatography-mass spectrometry. *Science Journal of Analytical Chemistry* 4(4): 42-51.
20. Trivedi MK, Branton A, Trivedi D, Nayak G, Panda P, et al. (2016) Mass spectrometric analysis of isotopic abundance ratio in biofield energy treated thymol. *Frontiers in Applied Chemistry* 1(1): 1-8.
21. Trivedi MK, Tallapragada RM, Branton A, Trivedi D, Nayak G, et al. (2015) Potential impact of biofield treatment on atomic and physical characteristics of magnesium. *Vitam Miner* 4(3): 1-6.
22. Trivedi MK, Tallapragada RM, Branton A, Trivedi D, Nayak G, et al. (2015) Evaluation of biofield energy treatment on physical and thermal characteristics of selenium powder. *Journal of Food and Nutrition Sciences* 3(6): 223-228.
23. Trivedi MK, Branton A, Trivedi D, Nayak G, Saikia G, et al. (2015) Physical and structural characterization of biofield treated imidazole derivatives. *Nat Prod Chem Res* 3(5): 1-8.
24. Trivedi MK, Branton A, Trivedi D, Nayak G, Bairwa K, et al. (2015) Spectroscopic characterization of disulfiram and nicotinic acid after biofield treatment. *J Anal Bioanal Tech* 6(5): 265.
25. Trivedi MK, Patil S, Shettigar H, Mondal SC, Jana S (2015) The potential impact of biofield treatment on human brain tumor cells: A time-lapse video microscopy. *J Integr Oncol* 4(3): 1-4.
26. Trivedi MK, Patil S, Shettigar H, Gangwar M, Jana S (2015) *In Vitro* evaluation of biofield treatment on cancer biomarkers involved in endometrial and prostate cancer cell lines. *J Cancer Sci Ther* 7(7): 253-257.
27. Trivedi MK, Patil S, Shettigar H, Mondal SC, Jana S (2015) Evaluation of biofield modality on viral load of Hepatitis B and C viruses. *J Antivir Antiretrovir* 7(3): 83-88.
28. Trivedi MK, Patil S, Shettigar H, Mondal SC, Jana S (2015) *In vitro* evaluation of biofield treatment on enterobacter cloacae: Impact on antimicrobial susceptibility and biotype. *J Bacteriol Parasitol* 6(5): 1-6.
29. Trivedi MK, Branton A, Trivedi D, Nayak G, Gangwar M, et al. (2015) Agronomic characteristics, growth analysis, and yield response of biofield treated mustard, cowpea, horse gram, and groundnuts. *International Journal of Genetics and Genomics*. 3(6): 74-80.
30. Trivedi MK, Branton A, Trivedi D, Nayak G, Mondal SC, et al. (2015) Evaluation of plant growth, yield and yield attributes of biofield energy treated mustard (*Brassica juncea*) and chick pea (*Cicer Arietinum*) Seeds. *Agriculture, Forestry and Fisheries* 4(6): 291-295.
31. MiniFlex (1997) Desktop X-ray Diffractometer. *The Rigaku Journal* 14(1): 29-36.
32. Zhang T, Paluch K, Scalabrino G, Frankish N, Healy AM, et al. (2015) Molecular structure studies of (1S,2S)-2-benzyl-2,3-dihydro-2-(1Hinden-2-yl)-1H-inden-1-ol. *J Mol Struct* 1083: 286-299.

33. Langford JJ, Wilson AJC (1978) Scherrer after sixty years: A survey and some new results in the determination of crystallite size. *J Appl Cryst* 11: 102-113.
34. Trivedi MK, Sethi KK, Panda P, Jana S (2017) A comprehensive physicochemical, thermal, and spectroscopic characterization of zinc (II) chloride using X-ray diffraction, particle size distribution, differential scanning calorimetry, thermogravimetric analysis/differential thermogravimetric analysis, ultraviolet-visible, and Fourier transform-infrared spectroscopy. *International Journal of Pharmaceutical Investigation* 7(1): 33-40.
35. Trivedi MK, Sethi KK, Panda P, Jana S (2017) Physicochemical, thermal and spectroscopic characterization of sodium selenate using XRD, PSD, DSC, TGA/DTG, UV-vis, and FT-IR. *Marmara Pharmaceutical Journal* 21(2): 311-318.
36. Inoue M, Hirasawa I (2013) The relationship between crystal morphology and XRD peak intensity on $\text{CaSO}_4 \cdot 2\text{H}_2\text{O}$. *J Crystal Growth* 380(1): 169-175.
37. Raza K, Kumar P, Ratan S, Malik R, Arora S (2014) Polymorphism: The phenomenon affecting the performance of drugs. *SOJ Pharm Pharm Sci* 1(2): 1-10.
38. Brittain HG (2009) Polymorphism in pharmaceutical solids. 2nd (Edn.), drugs and pharmaceutical sciences. Informa Healthcare USA, Inc., New York.
39. Censi R, Martino PD (2015) Polymorph impact on the bioavailability and stability of poorly soluble drugs. *Molecules* 20(910): 18759-18776.
40. Blagden N, de Matas M, Gavan PT, York P (2007) Crystal engineering of active pharmaceutical ingredients to improve solubility and dissolution rates. *Adv Drug Deliv Rev* 59(7): 617-630.
41. Mosharraf M, Nystrom C (1995) The effect of particle size and shape on the surface specific dissolution rate of microsized practically insoluble drugs. *Int J Pharm* 122(1-2): 35-47.
42. Buckton G, Beezer AE (1992) The relationship between particle size and solubility. *Int J Pharmaceutics* 82(3): R7-R10.

